Exosomes From Human Induced Pluripotent Stem Cells-derived Keratinocytes Accelerate Burn Wound Healing Through miR-762 Mediated Promotion of Keratinocytes and Endothelial Cells Migration

Yunyao Bo
Southern Medical University
Lijun Yang
Southern Medical University
Baiting Liu
Southern Medical University
Guiping Tian
Southern Medical University
Chenxi Li
Southern Medical University
Lin Zhang
Southern Medical University
Yuan Yan (yyuanmm@163.com)
Southern Medical University

Research Article

Keywords: Exosome, Burn, Induced pluripotent stem cells, Keratinocytes, Endothelial cell

Posted Date: January 27th, 2022

DOI: https://doi.org/10.21203/rs.3.rs-1289192/v1

Abstract

Background: The use of keratinocytes derived from induced pluripotent stem cells (iPSCs-KCs) may represent a novel cell therapy strategy for burn treatment. There is growing evidence that extracellular vesicles, including exosomes, are primary mediators of the benefits of stem cell therapy. Herein, we thus explored the effects of exosomes produced by iPSCs-derived keratinocytes (iPSCs-KCs-Exos) in a model of deep second-degree burn wound healing and evaluated the mechanistic basis for the observed activity.

Methods: iPSCs-KCs-Exos were isolated from conditioned medium of iPSCs-KCs and verified by electron micrograph and size distribution. Next, iPSCs-KCs-Exos were injected subcutaneously around wound sites, and its efficacy was evaluated by measuring wound closure areas, histological examination and immunohistochemistry staining. The effects of iPSCs-KCs-Exos on proliferation and migration of keratinocytes and endothelial cells *in vitro* were assessed by EdU staining, wound healing assays and transwell assay. Then, high-throughput microRNA sequencing was used to explore the underlying mechanisms. We assessed the roles of miR-762 in iPSCs-KCs-Exos-induced regulation of keratinocytes and endothelial cells migration. Furthermore, the target gene which mediated the biological effects of miR-762 in keratinocytes and endothelial cells was also been detected.

Results: The analysis revealed that iPSCs-KCs-Exos application to the burn wound drove the acceleration of wound closure, with more robust angiogenesis and re-epithelialization being evident. Such iPSCs-KCs-Exos treatment effectively enhanced endothelial cell and keratinocyte migration i*n vitro.* Moreover, the enrichment of miR-762 was detected in iPSCs-KCs-Exos and was found to target promyelocytic leukemia (PML) as a means of regulating cell migration through a mechanism tie to integrin beta1 (ITGB1).

Conclusion: These results thus provide a foundation for the further study of iPSCs-KCs-Exos as novel cell-free treatments for deep second-degree burns.

Introduction

Burns are a form of serious traumatic injury that cause substantial global morbidity, and there is thus an urgent need to define novel approaches to expediting burn healing [1–3]. Preclinical and clinical evidence suggests that keratinocyte-based therapies offer great promise in the context of burn management [4–6]. However, there are substantial challenges to large-scale keratinocyte preparation efforts owing to the fact that donor keratinocyte yields are often very limited. The ability of these donated cells to proliferate and differentiate *in vitro* is also highly variable. The Yamananka lab first developed induced pluripotent stem cells (iPSCs) and highlighted their potential as a novel source of many cellular lineages for use in therapeutic contexts [7–9]. The generated iPSCs are extremely similar to embryonic stem cells being capable of generating all cell lineages of different tissues including skin, highlighting a novel method of improving cell-based wound treatment efforts while minimizing ethical concerns and the risk of immune-mediated graft rejection [10, 11].

We have previously shown that iPSCs-derived keratinocytes (iPSCs-KCs) hold great promise for treating wound healing [12, 13]. However, the safety profile of these cells is not known and they are potentially limited by the risk of immunogenicity and genetic instability. Recent work has suggested that small membrane-bound exosomes derived from cells can facilitate a substantial fraction of the paracrine signaling necessary to facilitate intracellular communication [14, 15]. Exosomes of stem cells including bone marrow mesenchymal stem cells, human adipose stem cells, human amniotic epithelial cells and iPSCs can play an anti-inflammatory and anti-fibrosis role, inhibit oxidative stress and enhance angiogenesis, thus promoting skin wound healing [16–20]. As such, we speculate that iPSCs-KCs-derived exosomes (iPSCs-KCs-Eoxs) have the potential to play a direct role in the facilitation of burn wound healing. Up to now, there are no related studies on the iPSCs-KCs-Exos, and there are few studies on the primary keratinocyte's exosomes in skin wound healing [21–23].

Herein, we utilized iPSCs-KCs-Exos to treat murine skin wounds in order to test the therapeutic efficacy of these cell-free vesicles. We found that such iPSCs-KCs-Exos treatment was conducive to more rapid wound closure as well as enhanced endothelial cell and keratinocyte migration. We then evaluated the microRNAs present within these exosomes in an effort to identify important mediators of this wound healing phenotype, and found miR-762 to be highly enriched in iPSCs-KCs-Exos and to serve as an important mediator of cellular migration owing to its ability to target PML. Overall, these data highlight the important roles played by iPSCs-KCs-Exos and miR-762 in the treatment of cutaneous wounds.

Materials And Methods

Cell culture

The human iPS cell line was provided by Stem Cell Bank, Chinese Academy of Sciences. hiPSCs were cultured on Matrigel (BD Biosciences, CA) in mTeSR^{TM}1 medium (Stemcell Technologies, CA) and passaged every 4-7 days. hiPSCs were induced to keratinocytes as described previously [11]. Briefly, hiPSCs were switched to unconditioned medium (UM) supplemented with retinoic acid (RA): DMEM/F12 containing 20% knockout serum replacer, 1mM L-glutamine, 1× MEM nonessential amino acids, 0.1 mM b-mercaptoethanol (all from Life Technologies, USA) and 1 mM all-trans RA (Sigma-Aldrich, USA). Cells were cultured in UM+RA for 7 days, changing medium daily. On day 8, cells were passaged onto gelatin-coated plates in Keratinocyte Defined Serum-free Medium (K-DSFM, Life Technologies). After 4 weeks, differentiated cells were subcultured using trypsin to obtain high purity keratinocytes populations. Terminal differentiation was induced by adding 1.5 mM $CaCl_2$ in K-DSFM for 10 days. HaCaT cells were cultured in Dulbecco's modified Eagle's medium (DMEM, Gibco, USA), supplemented with 10% fetal bovine serum (Gibico, USA). Human umbilical cord samples were collected from patients with informed consent. The middle part of the human umbilical cord vein was cut into small segments, and the residual blood was cleaned with PBS. Collagenase Ⅱ was added into the segments. After digestion for 15 minutes, the lysis solution was sucked out and added into ECM medium for primary culture. Human umbilical vein endothelial cells (HUVECs) from the third passages were used. HaCaT cells and HUVECs were transfected

with PML overexpression plasmid (pcDNA3.1-PML), PML siRNA, and miR-762 mimics using Lipofectamine 2000 (Invitrogen, USA) according to the manufacturer's instructions.

Extraction and identification of iPSCs-KCs-Exos

iPSCs-KCs were cultured in K-DSFM for 48 h. After collecting the supernatant, exosomes were isolated and purified by serial ultracentrifugation, using ultracentrifuge (Beckman, Germany). The exosomes was suspended in PBS. Concentration of exosomes was measured by Enhanced BCA Protein Assay Kit (Beyotime, China). Then, transmission electron microscopy (TEM) was used to observe the morphological structure of exosomes. Size distribution and concentration of iPSCs-KCs-Exos were analyzed by nano-particle tracking analysis (NTA) using Nanosight LM 10 (Malvern Panalytical, UK).

Treatment of deep second-degree burns

The 8-week-old C57BL/6 mice were purchased from the Experimental Animal Center of Southern Medical University. After the hair removal from the back of mice, the opening at one end of a cylindrical plastic tube with a diameter of 1.5 cm was affixed to the back skin of mice. Then pour boiling water into the tube at a height of 2 cm and then the tube was removed after 18 seconds. After burn, local subcutaneous injections of PBS or exosomes were given to the wound site.

Histological observations

The skin tissues were fixed with 4% paraformaldehyde for 72 h, embedded in paraffin, and then cut into 5 mm thick sections. The sections were stained with hematoxylin eosin (H&E) staining (Leagene, China) and Masson's tri-chrome staining (MXB Biotechnologies, China). The re-epithelialization was calculated in the accordance with the formula [distance of the re-epithelium]/ [distance of the wound] ×100.

Immunofluorescence assay

At room temperature, cells were fixed with 4% paraformaldehyde for 30 min and then drilled with 0.5% Triton X-100 for 15 minutes. The cells were incubated overnight at 4°C with primary antibodies against K14, loricrin or involucrin (Proteintech, USA) and then incubated with Alexa Fluor 647-conjugated sheep anti-rabbit second antibody (Abcam, UK) for 1 h at room temperature. DAPI (500 ng/mL) was used to stain nuclei. Fluorescence was observed under an inverted fluorescence microscope (Leica, Germany)

EDU staining

After cells were treated for 48 h, EdU was added to the culture medium and incubated for 4 h. The cells were fixed with 4% paraformaldehyde and then drilled with 0.5% Triton X-100 for 15 minutes. Then, the cells were stained using Beyoclick™ EDU cell proliferation kit Alexa Fluor 488 (Beyotime, China) and imaged using an inverted fluorescence microscope (Leica, Germany).

Wound healing assay

Cells were seeded into 24-well plates and cultured overnight. After each well was filled with 95% monolayer of cells, the tip of the 200 μL pipette was used to form linear scratch wounds. At 0 h and 24 h, the wound healing was recorded by a microscope (Leica, Germany). Image J software was used to quantitatively evaluate the wound healing rate.

Transwell assay

200 μL cell suspension (serum-free DMEM) was added to the upper chamber of Transwell, and 600 μL DMEM containing 2% FBS was added to the lower chamber. After 24 h incubation at 5% CO_2 and 37°C, the cells were fixed with 4% paraformaldehyde. The cells at the lower side of the membrane were stained with Crystal Violet Staining Solution (Beyotime China) for 15 min. An inverted microscope (Leica, Germany) randomly collected 10 images from each sample.

miRNA microarray analysis

miRNA microarray analysis was performed by Epibiotek (Guangzhou, China) as previously described [19].

Western blot analysis

The Western blot assay was performed as previously described [19]. Antibodies used were described as follow: anti-PML, anti-ITGB1or anti β-actin (all from Abcam, UK).

Reverse transcription quantitative polymerase chain (qRT-PCR)

Trizol™ reagent (Invitrogen, USA) was used to extract the total RNA from cells, according to the manufacturer's instructions. RNA was reverse-transcribed using RevertAid First Strand cDNA Synthesis Kit (Thermo Scientific, USA). qRT-PCR analysis was using ACEQ Universal SYBR qPCR Master Mix (Vazyme, China). Midtect A TrackTM miRNA qRT-PCR Starter Kit (RiboBio, China) was used for synthesis of miRNA cDNA. Then, Midtect A TrackTM miRNA qRT-PCR Starter Kit (RiboBio, China) were used for qRT-PCR.

Luciferase report assay

The wild type and mutant miR-762 binding sites of PML 3'UTR sequence were subcloned into psiCHECK-2 vector. MiR-762 mimics or negative control mimics were co-transfected with recombinant plasmid into HEK-293 T cells using Lipofectamine 2000 (Invitrogen, USA). According to the manufacturer's instructions, the Firefly and Renilla luciferase activities were detected by Dual Luciferase Reporter Gene Assay Kit (Beyotime, China).

Statistical analysis

Data were presented as mean ± standard deviation (SD) of at least three independent experiments ($n \geq 3$). Statistical analysis was performed by independent samples *t*-test for comparison between two groups or one-way ANOVA among the groups. $p < 0.05$ was considered statistically significant.

Results

Characterization of iPSCs-KCs and iPSCs-KCs-Exos.

To characterize prepared iPSCs-KCs, we conducted immunohistochemical (IHC) staining for cytokeratin-14 (K14), which is a keratin marker confirming commitment of the ectoderm to a keratinocyte fate. As shown as in Fig. 1A, K14 was detectable in iPSCs-KCs. In addition, these $K14^+$ cells expressed involucrin and loricrin (Fig. 1B), markers of terminal epidermal differentiation, after induced differentiation in high calcium medium (1.5 mM $CaCl_2$), indicating that these iPSCs-KCs have the ability of epidermal differentiation.

Next, iPSCs-KCs-Exos preparations were characterized by ultracentrifuging iPSCs-KCs culture supernatants and analyzing them via transmission electron microscopy (TEM), revealing the presence of exosomes with the expected cup-shaped morphology (Fig. 1C). Nanoparticle tracking analysis (NTA) revealed these particles to have an average diameter of 75 nm (Fig. 1D). All these data suggested that these nanoparticles were actually exosomes.

iPSCs-KCs-Exos treatment accelerates the healing of deep second-degree burn in mice

To test the effects of iPSCs-KCs-Exos treatment on the healing of burn wounds, deep second-degree burns were generated in the abdominal skin of model mice, after which iPSCs-KCs-Exos or an equivalent volume of PBS was locally injected into these areas. Beginning on day 7 post-wounding, significant decreases in wound area in the iPSCs-KCs-Exos group were evident relative to the PBS group, and these improvements grew through day 11 (Fig. 2A). This suggests that iPSCs-KCs-Exos can promote the acceleration of cutaneous wound repair *in vivo.*

We additionally conducted histological analyses of these healing wounds. Improved re-epithelialization of the wound site was observed in the iPSCs-KCs-Exos treatment group on days 7 and 11 after wounding as compared to the control group when H&E staining was conducted (Fig. 2B, C). Furthermore, there was a significant increase in the length of epithelial tongues on days 7 and 11 in the iPSCs-KCs-Exos group compared to the PBS group (Fig. 2B, D). Immunohistochemical staining for CD31 further revealed that significant improvements in capillary density were evident in the iPSCs-KCs-Exos-treated wounds. (Fig. 2E). However, no differences in collagen deposition were observed when comparing iPSCs-KCs-Exos and PBS group (Fig. 2F). Together, these data revealed a role for iPSCs-KCs-Exos as drivers of re-epithelialization and angiogenesis, thereby enabling them to accelerate the wound healing process.

iPSCs-KCs-Exos promote the migration of keratinocytes and endothelial cells in vitro

To better elucidate the mechanisms where by iPSCs-KCs-Exos treatment can accelerate the burn wound healing, the impact of these exosomes on healing-related cell types (endothelial cells and keratinocytes) was next assessed. EdU assays were applied to determine the effect of iPSCs-KCs-Exos on the proliferation of these two kinds of cells. As shown as in Fig. 3A and B, these iPSCs-KCs-Exos did not alter

keratinocytes or HUVECs proliferation at all doses *in vitro.* In a wound healing assay, iPSCs-KCs-Exos treatment was associated with a significantly increased wound closure rate compared to PBS at doses of 1, 2, and 4 μg/ml (Fig. 2C). When evaluated using Transwell assays, HUVECs migratory activity was also found to be significantly increased following iPSCs-KCs-Exos treatment at doses of 1, 2, and 4 μg/ml (Fig. 2D). As such, iPSCs-KCs-Exos can enhance the migration of endothelial cells and keratinocytes migration without altering the proliferative activity of these cells.

miR-762 is enriched within iPSCs-KCs-Eoxs and serves as a key mediator of iPSCs-KCs-Exos-induced migration of keratinocytes and endothelial cells

While microRNAs (miRNAs) account for a relatively small fraction of the total content within extracellular vesicles, they have nonetheless been shown to be important modulators of cellular function [24]. To test the potential relevance of such miRNAs in the context of iPSCs-KCs-Exos-induced migratory activity and wound healing, miRNA microarray analysis was conducted using these exosomes. The result showed that miR-762 was the most abundant miRNA among these detected miRNAs (Table 1). Thus, we focused on exosomal miR-762 for next investigation. In a wound healing assay with HaCaT cells, the overexpression of miR-762 resulted in enhanced wound closure rates at 24 h post-wounding (Fig. 4A). To further confirm the functional importance of this miRNA, iPSCs-KCs-Exos-treated HaCaT cells were treated with a specific inhibitor of miR-762, which attenuated this enhanced migratory activity (Fig. 4A). The same effect was also observed in HUVECs (Fig. 4B). In addition, the expression of miR-762 in HaCaT cells and HUVECs was indeed significantly elevated at 48 h post-iPSCs-KCs-Exos treatment, confirming the ability of these exosomes to deliver miR-762 to recipient cells (Fig. 4C). These data thus suggest that miR-762 is an important mediator of iPSCs-KCs-Exos-induced migration of keratinocyte and endothelial cells *in vitro.*

miR-762 targets PML to regulate the migratory activity of keratinocytes and endothelial cells through ITGB1

To further clarify the regulatory role of iPSCs-KCs-Exos-derived miR-762 in the context of wound healing, potential target genes for this miRNA were next identified using the Targetscan, miRDB, and microRNA.org databases. This approach identified PML as a putative target of this miRNA. To confirm this prediction, luciferase reporter constructs containing wild-type (WT) or mutated (MUT) versions of the putative miR-762 binding site located within the PML 3’-untranslated region (UTR) were prepared (Fig. 5A). When 293T cells were transfected with these reporters and miR-762 mimics, this miRNA was confirmed to suppress the activity of the WT but not the MUT reporter, confirming the predicted regulatory relationship (Fig. 5B). Moreover, mRNA and protein levels of PML were significantly lower in HaCaT cells and HUVECs following miR-762 mimic or iPSCs-KCs-Exos treatment (Fig. 5C, D). PML is thus a direct miR-762 target gene. To further examine the link between PML downregulation and the effects of miR-762 and iPSCs-KCs-Exos on the migration of keratinocytes and endothelial cells, the PML was overexpressed with pcDNA3.1 vector. As shown as in Fig. 5E, overexpression of PML inhibited the migration of HaCaT cells and could restraine the cell migration that was promoted by miR-762 mimics or iPSCs-KCs-Exos.

The similar results were also observed in HUVECs (Fig. 5F). Taken together, above results suggest that miR-762 and iPSCs-KCs-Exos induced acceleration of keratinocytes and endothelial cells is mediated at least partly by inhibiting PML expression.

PML regulated ITGB1 is involved in the promotion of keratinocytes and endothelial cells migration by miR-762 and iPSCs-KCs-Exos.

Reineke et al. previously demonstrated that ITGB1 was responsible for mediating PML-induced changes in migratory activity [25]. In this study, we examined the effects of PML knockdown on ITGB1 expression by siRNA. When PML expression decreased, we observed an increase in ITGB1 mRNA and protein expression in keratinocytes and endothelial cells (Fig. 6A, B). We further found that the expression of ITGB1 also increased after treatment with miR-762 mimic or iPSCs-KCs-Eoxs (Fig. 6C, D). Moreover, siRNA-mediated ITGB1 knockdown ablated the miR-762 mimic and iPSCs-KCs-Eoxs induced migration of HaCaT cells and HUVECs (Fig. 6E, F). Together, these data suggest that miR-762 can target PML to enhance the migration of keratinocyte and endothelial cells through a mechanism involving ITGB1.

Discussion

Herein, we found that iPSCs-KCs-Exos treatment was sufficient to promote keratinocyte migration and to thereby accelerate the healing of deep second-degree burn wounds in mice. We additionally determined that the most abundant miRNA within these exosomes, miR-762, was a key mediator of this enhanced migratory effect owing to its ability to target PML.

In the process of wound healing, keratinocytes, fibroblasts and endothelial cells are the main cell populations involved in re-epithelialization and granulation tissue construction [26]. Therefore, communication between these cells plays a key role in skin repair. This network is likely regulated by cell-derived exosomes, which carry a range of macromolecular cargos that can be delivered to target cells, enabling them to regulate recipient cell responses in a variety of complex manners [14, 15]. Both HaCaT cells and primary keratinocytes can release exosomes and other extracellular vesicles [27, 28]. In their deep sequencing analysis of microRNAs within keratinocyte-derived extracellular vesicles, Than et al. found that the most enriched miRNAs found therein were linked to key physiological processes such as fibroblast migration and dermal-epithermal wound healing, suggesting a role for these vesicles in the context of cutaneous wound healing [21].

This study was designed to explore the ability of iPSC-KC-derived exosomes to regulate the process of burn wound healing. We successfully generated and characterized iPSCs-KCs-Exos, which were of the expected size and exhibited characteristic morphological features. Cutaneous wound healing processes are complicated and necessitate interplay between inflammatory, angiogenic, remodeling, proliferative, epithelialization, and fibrotic processes [29]. Histological analyses revealed that increases in re-epithelialization and capillary density were evident in wound sites following iPSCs-KCs-Exos treatment, but collagen formation was not affected. Thus, we then further examined the effects of these exosomes on endothelial cells and keratinocytes, which are the key mediators of angiogenesis and epithelialization,

respectively. These analyses revealed that iPSCs-KCs-Exos significantly enhanced the migratory activity of these cells without impacting their proliferative activity. As such, the beneficial impact of these exosomes in the context of cutaneous wound healing may be primarily attributable to their ability to promote keratinocyte and endothelial cell migration.

Exosomes contain a variety of miRNAs, mRNAs, lipids, and proteins that are compiled within the ExoCarta database [14, 15]. Of these, miRNAs are the best-studied exosomal cargos owing to their ability to regulate target mRNA expression. Herein, we detected many miRNAs that were highly abundant within iPSCs-KCs-Exos, of which miR-762 was detected at the highest levels. Moreover, we found that miR-762 was able to promote endothelial cell and keratinocyte migration in a manner similar to iPSCs-KCs-Exos treatment, suggesting that it is likely a primary mediator of the phenotypic effects-KCs-Exos in the context of wound healing. In prior research, miR-762 has been found to regulate a range of target genes in different contexts. The upregulation of miR-762 in non-small cell lung cancer, bladder cancer, breast cancer and nasopharyngeal carcinoma has been linked to enhanced tumor cell invasivity, migration, and proliferation [30–33]. However, there have been no prior studies regarding the role of this specific miRNA in keratinocytes or endothelial cells. In line with these past findings, we observed a pro-migratory role for miR-762 in both of these cell types.

Herein, we identified promyelocytic leukemia (PML) as a novel miR-762 target gene associated with the ability of this miRNA to regulate endothelial cell and keratinocyte migration. PML plays a role in a number of important cellular processes, including tumor suppression, apoptosis, transcriptional regulation, DNA damage response, senescence and viral defense mechanisms [34–36]. Herein, we confirmed that PML was a direct miR-762 target, and we found that overexpressing PML was sufficient to reverse the beneficial impact of miR-762 on cellular migration. In prior reports, the ability of PML to suppress the migration of MDA-MB-231 cells was attributed to its ability to promote ITGB1 downregulation [25]. ITGB1 are important for attachment to and integrity of cell-extracellular matrix (BME) interaction by mediating binding to BME components, and they are generally required for migration of keratinocytes and endothelial cells [37, 38]. We thus explored the link between ITGB1 and this miR-762/PML regulatory axis, leading us to conclude that PML overexpression suppressed ITGB1 expression while miR-762 was able to reverse this effect. We further confirmed a role for ITGB1 in the miR-762/PML-mediated migratory phenotypes observed in this experimental system. However, as miRNAs target multiple genes, these results do not offer any insight into the ability of miR-762 to regulate other signaling pathways within keratinocytes. Moreover, while PML and ITGB1 clearly play a role in this process, further work is required to elucidate the underlying mechanisms.

In conclusion, these results indicate that iPSCs-KCs-Exos treatments can significantly improve burn wound healing outcomes, highlighting novel approaches to expediting cutaneous wound healing and providing a foundation for future research efforts.

Abbreviations

iPSCs: induced pluripotent stem cells; iPSCs-KCs: iPSCs-derived keratinocytes; iPSCs-KCs-Exos: iPSCs-KCs-derived exosomes; PML: promyelocytic leukemia; integrin beta1 (ITGB1); UM: unconditioned medium; RA: retinoic acid; K-DSFM: keratinocyte defined serum-free Medium; DMEM: Dulbecco's modified eagle's medium; HUVECs: human umbilical vein endothelial cells; PBS: phosphate-buffered saline; TEM: transmission electron microscopy; NTA: nanoparticle tracking analysis; H&E: hematoxylin and eosin; DAPI: 4,6-diamidino-2-phenylindole; EdU: 5-Ethynyl-2'-deoxyuridine; qRT-PCR: quantitative real-time polymerase chain reaction; K14: cytokeratin-14; miRNAs: microRNAs; BME: cell-extracellular matrix.

Declarations

Acknowledgements

Not applicable.

Authors' Contributions

LZ and YY participated in all aspects of the study, including design, financial support, analyses, final approval of manuscript and revised the manuscript. YY B and LJ Y performed the experimental work and analyzed the data. BT L, GP T and CX L performed the collection and/or assembly of data and revised the manuscript; All authors agreed to be accountable for all aspects of the work.

Funding

This work was funded by the National Natural Science Foundation of China (No: 82072186, No: 81872514).

Availability of data and materials

The authors agree to share data and materials related to this manuscript.

Ethics approval and consent to participate

The Bioethics Committee of Southern Medical University approved all animal procedures, which were in accordance with the National Institutes of Health (NIH) Guide for the Care and Use of Laboratory Animals.

Consent for publication

Not applicable.

Competing Interests

The authors declared no potential conflicts of interest.

References

1. Jeschke MG, van Baar ME, Choudhry MA et al. Nat Rev Dis Primers 2020 Feb 13;6(1):11.
2. Nielson CB, Duethman NC, Howard JM et al. Burns: Pathophysiology of Systemic Complications and Current Management. J Burn Care Res. 2017 Jan/Feb;38(1):e469-e481.
3. Roshangar L, Soleimani Rad J, Kheirjou R et al. Skin Burns: Review of Molecular Mechanisms and Therapeutic Approaches. Wounds. 2019 Dec;31(12):308-315.
4. Ter Horst B, Chouhan G, Moiemen NS et al. Advances in keratinocyte delivery in burn wound care. Adv Drug Deliv Rev. 2018 Jan 1;123:18-32.
5. Rowan MP, Cancio LC, Elster EA et al. Burn wound healing and treatment: review and advancements. Crit Care. 2015 Jun 12;19:243.
6. Fang T, Lineaweaver WC, Sailes FC et al. Clinical application of cultured epithelial autografts on acellular dermal matrices in the treatment of extended burn injuries. Ann Plast Surg. 2014 Nov;73(5):509-515.
7. Takahashi K, Yamanaka S. Induction of pluripotent stem cells from mouse embryonic and adult fibroblast cultures by defined factors. Cell. 2006 Aug 25;126(4):663-676.
8. Talug B, Tokcaer-Keskin Z. Induced Pluripotent Stem Cells in Disease Modelling and Regeneration. Adv Exp Med Biol. 2019;1144:91-99.
9. Hu J, Wang J. From embryonic stem cells to induced pluripotent stem cells-Ready for clinical therapy? Clin Transplant. 2019 Jun;33(6):e13573.
10. Miyake T, Shimada M. 3D Organoid Culture Using Skin Keratinocytes Derived from Human Induced Pluripotent Stem Cells. Methods Mol Biol. 2021 Mar 11.
11. Selekman JA, Grundl NJ, Kolz JM et al. Efficient generation of functional epithelial and epidermal cells from human pluripotent stem cells under defined conditions. Tissue Eng Part C Methods. 2013 Dec;19(12):949-960.
12. Yan Y, Jiang J, Zhang M et al. Effect of iPSCs-derived keratinocytes on healing of full-thickness skin wounds in mice. Exp Cell Res. 2019 Dec 1;385(1):111627.
13. Wu R, Du D, Bo Y et al. Hsp90alpha promotes the migration of iPSCs-derived keratinocyte to accelerate deep second-degree burn wound healing in mice. Biochem Biophys Res Commun. 2019 Nov 26;520(1):145-151.
14. Kalluri R, LeBleu VS. The biology, function, and biomedical applications of exosomes. Science. 2020 Feb 7;367(6478):eaau6977.
15. Pegtel DM, Gould SJ. Exosomes. Annu Rev Biochem. 2019 Jun 20;88:487-514.
16. He L, Zhu C, Jia J et al. ADSC-Exos containing MALAT1 promotes wound healing by targeting miR-124 through activating Wnt/β-catenin pathway. Biosci Rep. 2020 May 29;40(5):BSR20192549.
17. Ren S, Chen J, Duscher D et al. Microvesicles from human adipose stem cells promote wound healing by optimizing cellular functions via AKT and ERK signaling pathways. Stem Cell Res Ther.

2019 Jan 31;10(1):47.
18. An Y, Lin S, Tan X et al. Exosomes from adipose-derived stem cells and application to skin wound healing. Cell Prolif. 2021 Mar;54(3):e12993.
19. Yan Y, Wu R, Bo Y et al. Induced pluripotent stem cells-derived microvesicles accelerate deep second-degree burn wound healing in mice through miR-16-5p-mediated promotion of keratinocytes migration. Theranostics. 2020 Aug 8;10(22):9970-9983.
20. Rani S, Ritter T. The Exosome - A Naturally Secreted Nanoparticle and its Application to Wound Healing. Adv Mater. 2016 Jul;28(27):5542-5552.
21. Than UTT, Guanzon D, Broadbent JA et al. Differential Expression of Keratinocyte-Derived Extracellular Vesicle Mirnas Discriminate Exosomes From Apoptotic Bodies and Microvesicles. Front Endocrinol (Lausanne). 2018 Sep 11;9:535.
22. Zhou X, Brown BA, Siegel AP et al. Exosome-Mediated Crosstalk between Keratinocytes and Macrophages in Cutaneous Wound Healing. ACS Nano. 2020 Oct 27;14(10):12732-12748.
23. Chavez-Muñoz C, Kilani RT, Ghahary A. Profile of exosomes related proteins released by differentiated and undifferentiated human keratinocytes. J Cell Physiol. 2009 Oct;221(1):221-231.
24. Yu X, Odenthal M, Fries JW. Exosomes as miRNA Carriers: Formation-Function-Future. Int J Mol Sci. 2016 Dec 2;17(12):2028.
25. Reineke EL, Liu Y, Kao HY. Promyelocytic leukemia protein controls cell migration in response to hydrogen peroxide and insulin-like growth factor-1. J Biol Chem. 2010 Mar 26;285(13):9485-9492.
26. Rodrigues M, Kosaric N, Bonham CA et al. Wound Healing: A Cellular Perspective. Physiol Rev. 2019 Jan 1;99(1):665-706.
27. Ogawa M, Udono M, Teruya K et al. Exosomes Derived from Fisetin-Treated Keratinocytes Mediate Hair Growth Promotion. Nutrients. 2021 Jun 18;13(6):2087.
28. Jiang M, Fang H, Shao S et al. Keratinocyte exosomes activate neutrophils and enhance skin inflammation in psoriasis. FASEB J. 2019 Dec;33(12):13241-13253.
29. Sorg H, Tilkorn DJ, Hager S et al. Skin Wound Healing: An Update on the Current Knowledge and Concepts. Eur Surg Res. 2017;58(1-2):81-94.
30. Ge P, Cao L, Chen X et al. miR-762 activation confers acquired resistance to gefitinib in non-small cell lung cancer. BMC Cancer. 2019 Dec 10;19(1):1203.
31. Liu T, Lu Q, Liu J et al. Circular RNA FAM114A2 suppresses progression of bladder cancer via regulating NP63 by sponging miR-762. Cell Death Dis. 2020 Jan 22;11(1):47.
32. Li Y, Huang R, Wang L et al. microRNA-762 promotes breast cancer cell proliferation and invasion by targeting IRF7 expression. Cell Prolif. 2015 Dec;48(6):643-649.
33. Bao LH, Ji K, Li D et al. The biological function and diagnostic value of miR-762 in nasopharyngeal carcinoma. J Chin Med Assoc. 2021 May 1;84(5):498-503.
34. Guan D, Kao HY. The function, regulation and therapeutic implications of the tumor suppressor protein, PML. Cell Biosci. 2015 Nov 4;5:60.

35. Jin G, Gao Y, Lin HK. Cytoplasmic PML: from molecular regulation to biological functions. J Cell Biochem. 2014 May;115(5):812-818.
36. Imani-Saber Z, Ghafouri-Fard S. Promyelocytic leukemia gene functions and roles in tumorigenesis. Asian Pac J Cancer Prev. 2014;15(19):8021-8028.
37. Koivisto L, Heino J, Häkkinen L et al. Integrins in Wound Healing. Adv Wound Care (New Rochelle). 2014 Dec 1;3(12):762-783.
38. Brakebusch C, Fässler R. beta 1 integrin function in vivo: adhesion, migration and more. Cancer Metastasis Rev. 2005 Sep;24(3):403-411.

Table

Table 1 Highly expressed miRNAs in iPSCs-KCs-Exos.

Gene ID	Name	Read count
MIMAT0010313	hsa-miR-762	115546
MIMAT0000266	hsa-miR-205-5p	114148
MIMAT0000067	hsa-let-7f-5p	91099
MIMAT0000069	hsa-miR-16-5p	51004
MIMAT0000086	hsa-miR-29a-3p	28959
MIMAT0000278	hsa-miR-221-3p	24733
MIMAT0000415	hsa-let-7i-5p	22310
MIMAT0000062	hsa-let-7a-5p	14970
MIMAT0000063	hsa-let-7b-5p	13934
MIMAT0005898	hsa-miR-1246	13716
MIMAT0000732	hsa-miR-378a-3p	13533
MIMAT0000076	hsa-miR-21-5p	13026
MIMAT0000259	hsa-miR-182-5p	12760
MIMAT0000281	hsa-miR-224-5p	11130
MIMAT0000083	hsa-miR-26b-5p	10781
MIMAT0000226	hsa-miR-196a-5p	9398
MIMAT0000764	hsa-miR-339-5p	9122
MIMAT0000078	hsa-miR-23a-3p	8538
MIMAT0049032	hsa-miR-12136	8013
MIMAT0000100	hsa-miR-29b-3p	6287
MIMAT0037311	hsa-miR-320a-5p	4900
MIMAT0000243	hsa-miR-148a-3p	4840
MIMAT0000082	hsa-miR-26a-5p	4421
MIMAT0000252	hsa-miR-7-5p	4384
MIMAT0000093	hsa-miR-93-5p	3581
MIMAT0000757	hsa-miR-151a-3p	3494
MIMAT0000074	hsa-miR-19b-3p	2943
MIMAT0000681	hsa-miR-29c-3p	2619

MIMAT0000419	hsa-miR-27b-3p	2593
MIMAT0000084	hsa-miR-27a-3p	2513

Figures

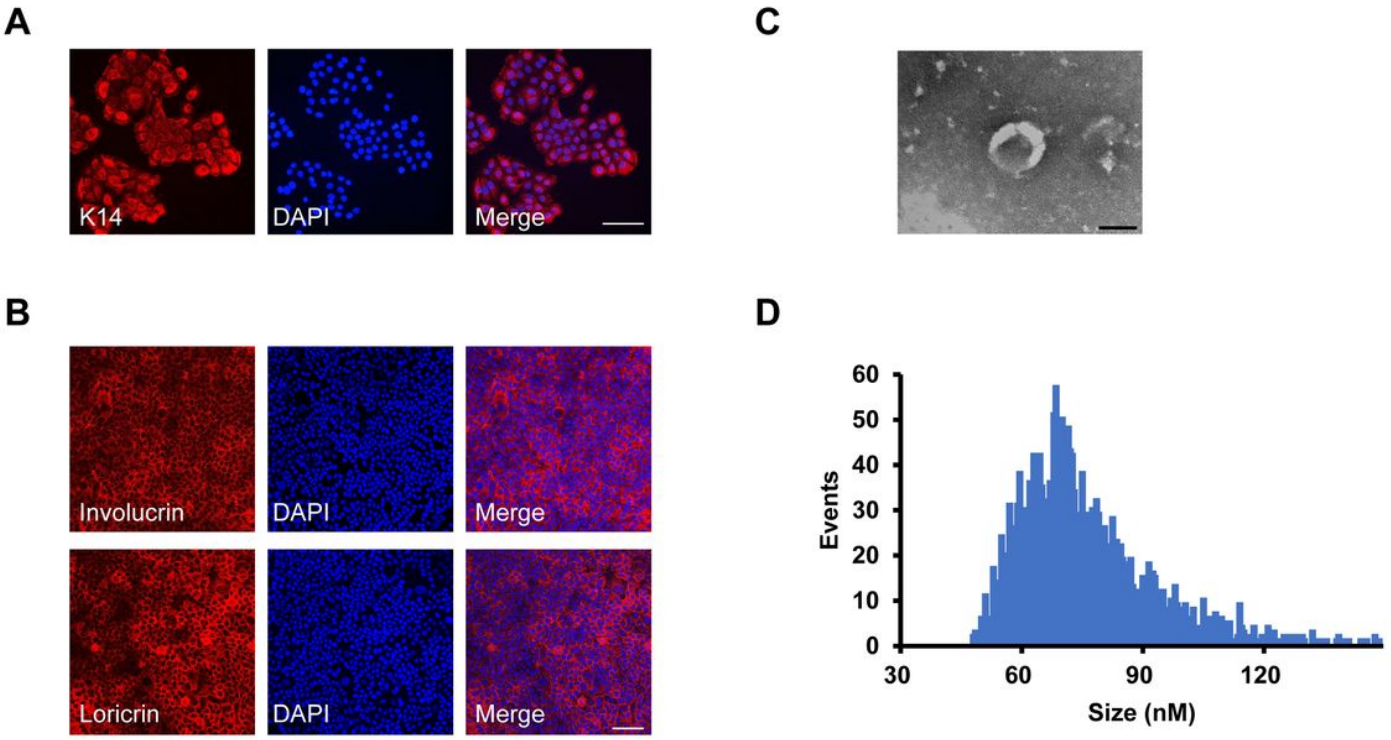

Figure 1

Characterization of iPSCs-KCs and iPSCs-KCs-Exos. (**A**) Representative images of immunohistochemical staining for K14 in iPSCs-KCs. Scale bar, 100 μm. (**B**) Representative images of immunohistochemical staining for involucrin and loricrin in iPSCs-KCs culture for 10 days in DKSFM supplemented with 1.5 mmol/L of $CaCl_2$. Scale bar, 100 μm. Nuclei was stained by DAPI (blue). (**C**) The transmission electron microscopy (TEM) image of iPSCs-KCs-Exos. Scale bar, 100 nm. (**D**) Nanoparticle tracking analysis (NTA) result of iPSCs-KCs-Exos.

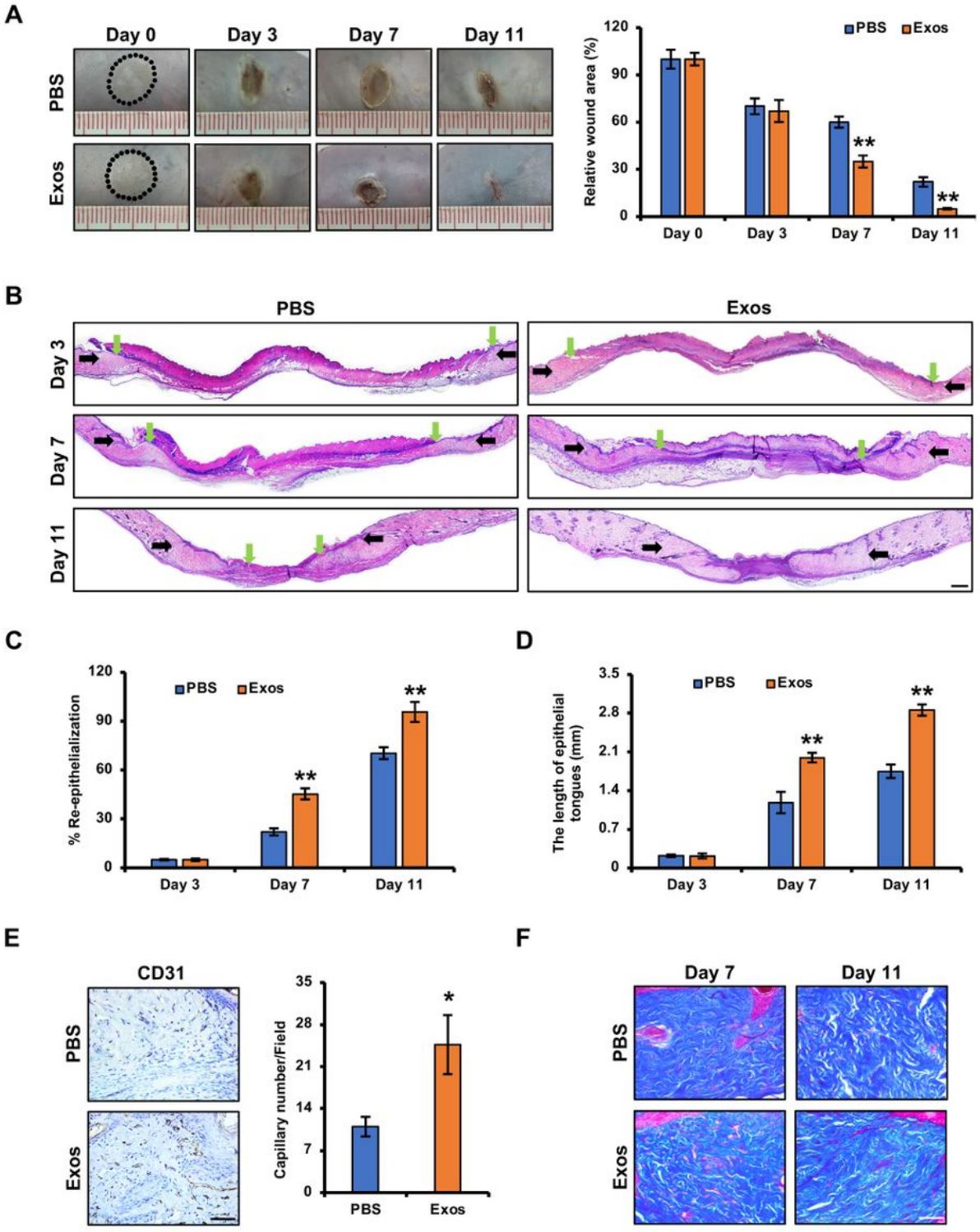

Figure 2

iPSCs-KCs-Exos accelerate deep second-degree burn wound healing *in vivo*. (**A**) Representative images of wounds treated with PBS or iPSCs-KCs-Exos on days 0, 3, 7 and 11 after burning and quantitative analysis of wound area in each group. (**B**) H&E staining of wounded skin sections treated with PBS or iPSCs-KCs-Exos on days 3, 7 and 11 after burning. Black arrows indicate the dermal border; green arrows indicate the epidermal margin. Scale bar, 400 μm. (**C**) Quantitative analysis of the re-epithelialization

ration of wounds in each group. (**D**) Quantitative analysis of the length of epithelial tongues of wounds in each group. (**E**) Immunohistochemistry staining for CD31 wounds and quantitative analysis of the numbers of stained capillaries in each group on days 11 after burning. Scale bar, 50 μm. (**F**) Masson's trichrome staining of wounds in each group on days 7 and 11 after burning. Scale bar, 50 μm. **P* < 0.05, ***P* < 0.01.

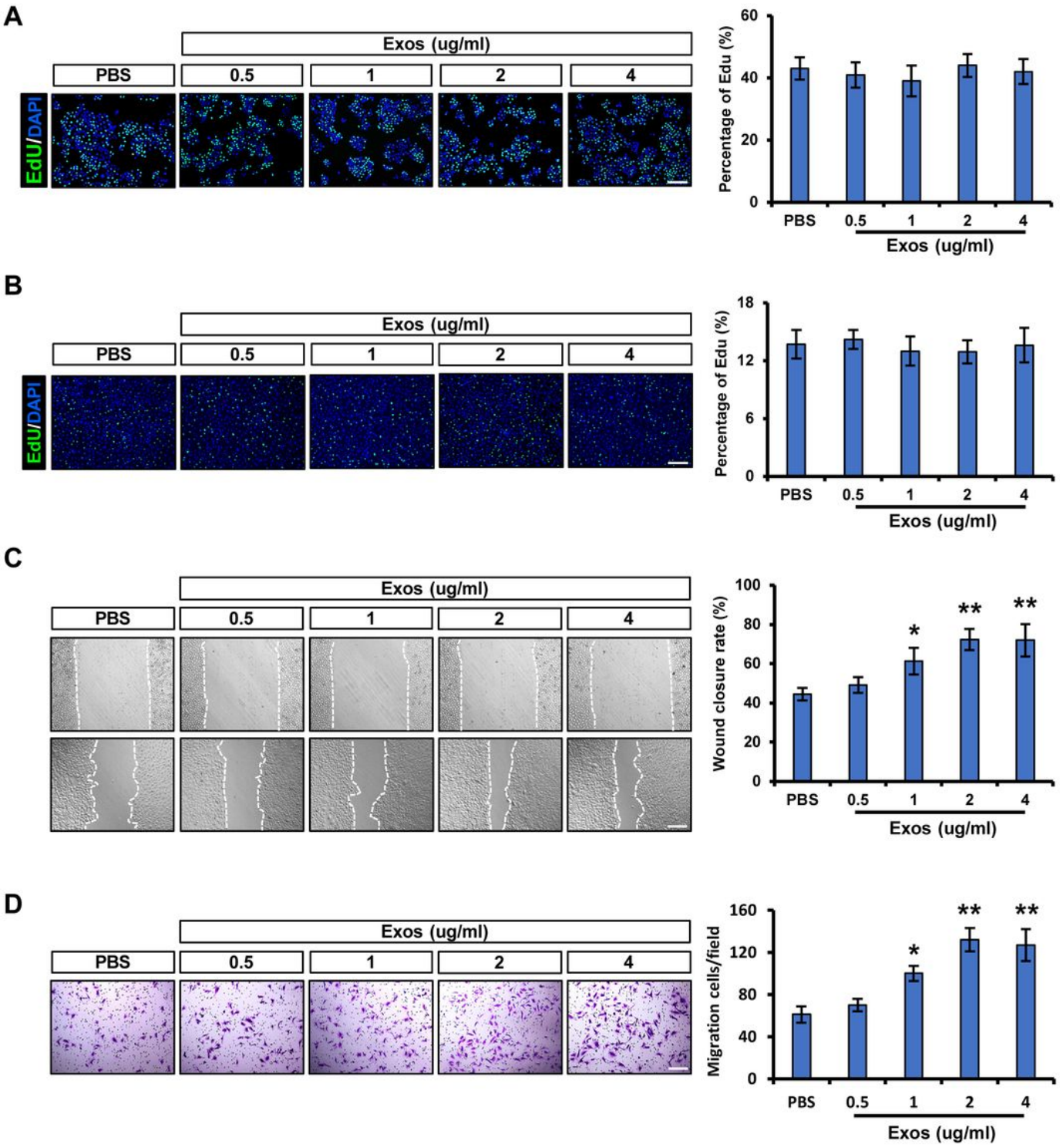

Figure 3

iPSCs-KCs-Exos promote the migration of keratinocytes and endothelial cells *in vitro*. (**A**) Representative fluorescence images of EdU staining of HaCaT cells treated with PBS or iPSCs-KCs-Exos (0.5, 1, 2, or 4 μg/mL) and quantitative analysis of the proliferation rates in each group. Scale bar, 200 μm. (**B**) Representative fluorescence images of EdU staining of HUVECs and quantitative analysis of the proliferation rates in each group. Scale bar, 200 μm. (**C**) Representative images of the wound healing assay and quantitative analysis of the wound healing rates in each group at 24 h. Scale bar, 200 μm. (**D**) Images of migrated HUVECs and quantitative analysis of the migrated cells in each group. Scale bar, 200 μm. *$P < 0.05$, **$P < 0.01$.

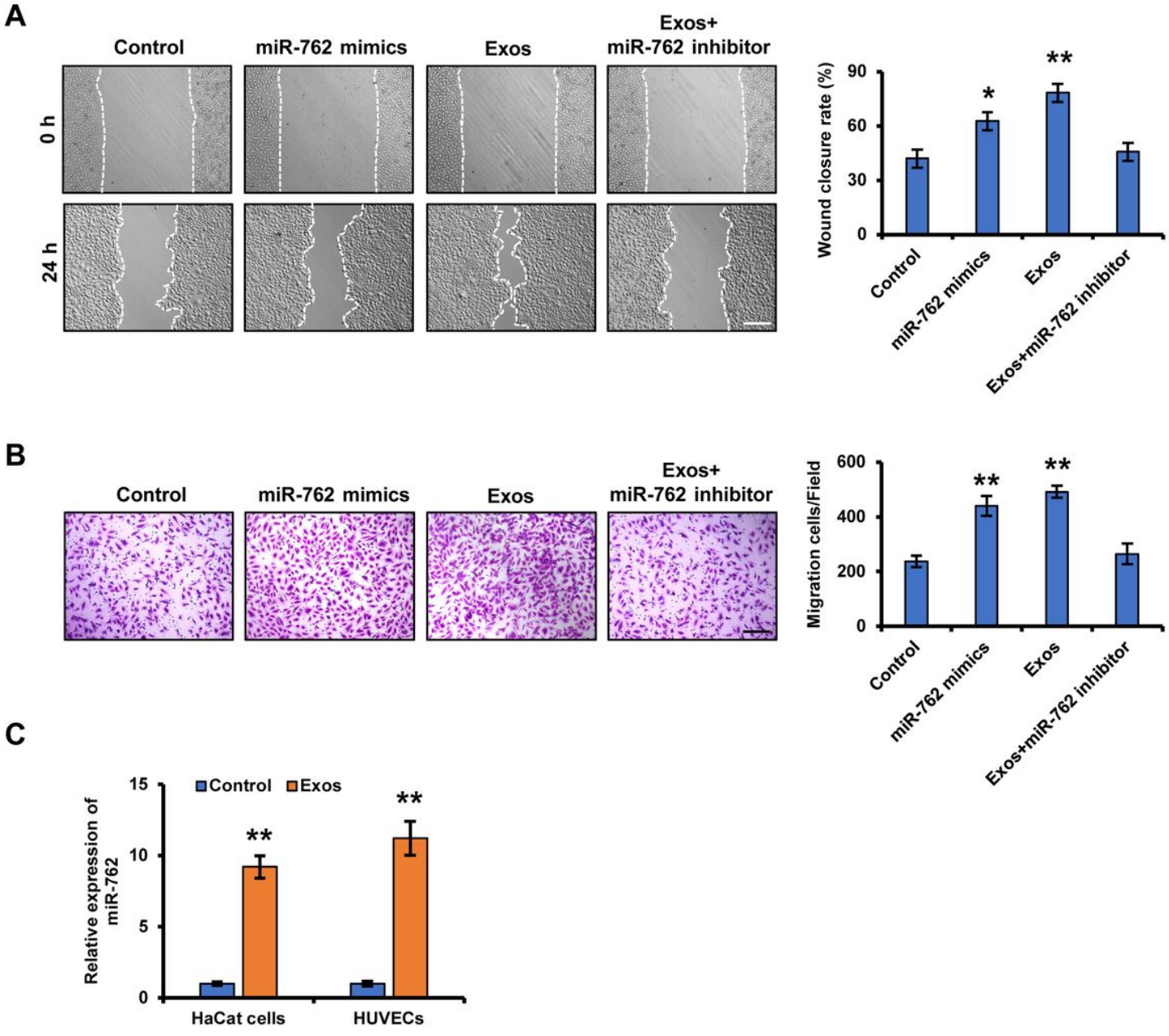

Figure 4

Mir-762 is a key mediator of iPSCs-KCs-Exos induced migration of keratinocytes and endothelial cells. (**A**) Representative images of the wound healing assay of keratinocytes in each group (left panel). Scale bar = 100 μm. Quantitative analysis of the wound healing rates in each group (right panel). (**B**) Images of migrated HUVECs in each group. Scale bar, 200 μm. Quantitative analysis of the migrated cells (right panel). Scale bar, 200 μm. (**C**) qRT-PCR analysis of miR-762 expression in HaCaT cells and HUVECs which were treated with iPSCs-KCs-Exos (2 μg/mL) for 24 h. **P* < 0.05, ***P* < 0.01.

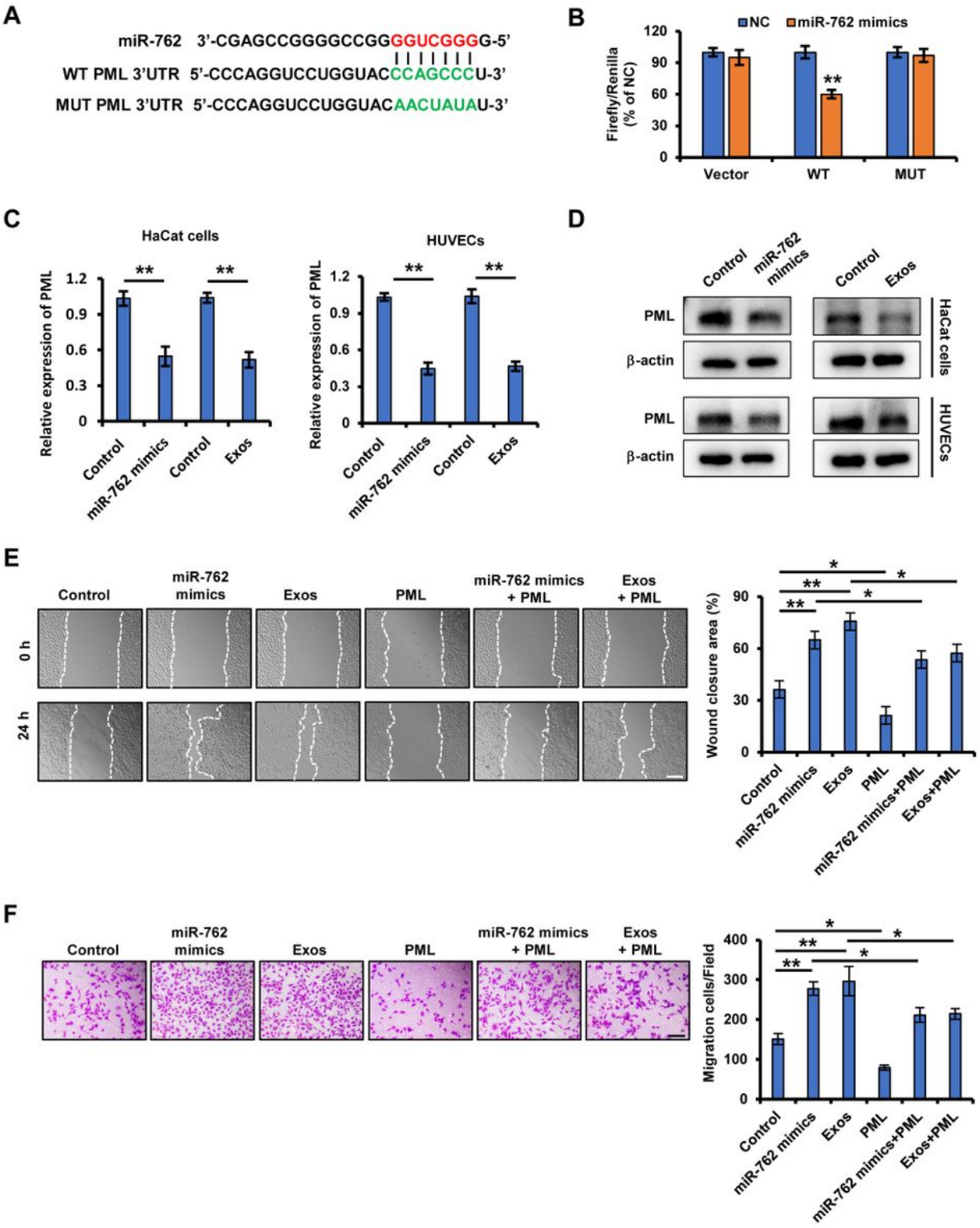

Figure 5

miR-762 and iPSCs-KCs-Exos promote migration of keratinocyte and endothelial cells by targeting PML. (**A**) Predicted miR-762 target sequences in PML 3'-UTR and the mutated nucleotides in the 3'UTR of PML. (**B**) The relative luciferase activity in 293T cells with psiCHECK-PML-wt-3'UTR (WT) or psiCHECK-PML-mut-3'UTR (MUT) and miR-762 mimics co-transfection was evaluated by luciferase reporter assay. qRT-PCR (**C**) and Western blot (**D**) analysis of PML expression in HaCaT cells and HUVECs which were treated with control, miR-762 mimics and iPSCs-KCs-Exos (Exos). (**E**) Representative images of the wound healing assay of HaCaT cells, which were treated with control, miR-762 mimics, iPSCs-KCs-Exos (Exos), pcDNA3.1-PML (PML), miR-762 mimic plus pcDNA3.1-PML (PML), iPSCs-KCs-Exos (Exos) plus pcDNA3.1-PML (PML) and quantitative analysis of the wound healing rates in each group. Scale bar, 200 μm. (**F**) Images of migrated HUVECs and quantitative analysis of the migrated cells in each group. Scale bar, 200 mm. *$P < 0.05$, **$P < 0.01$.

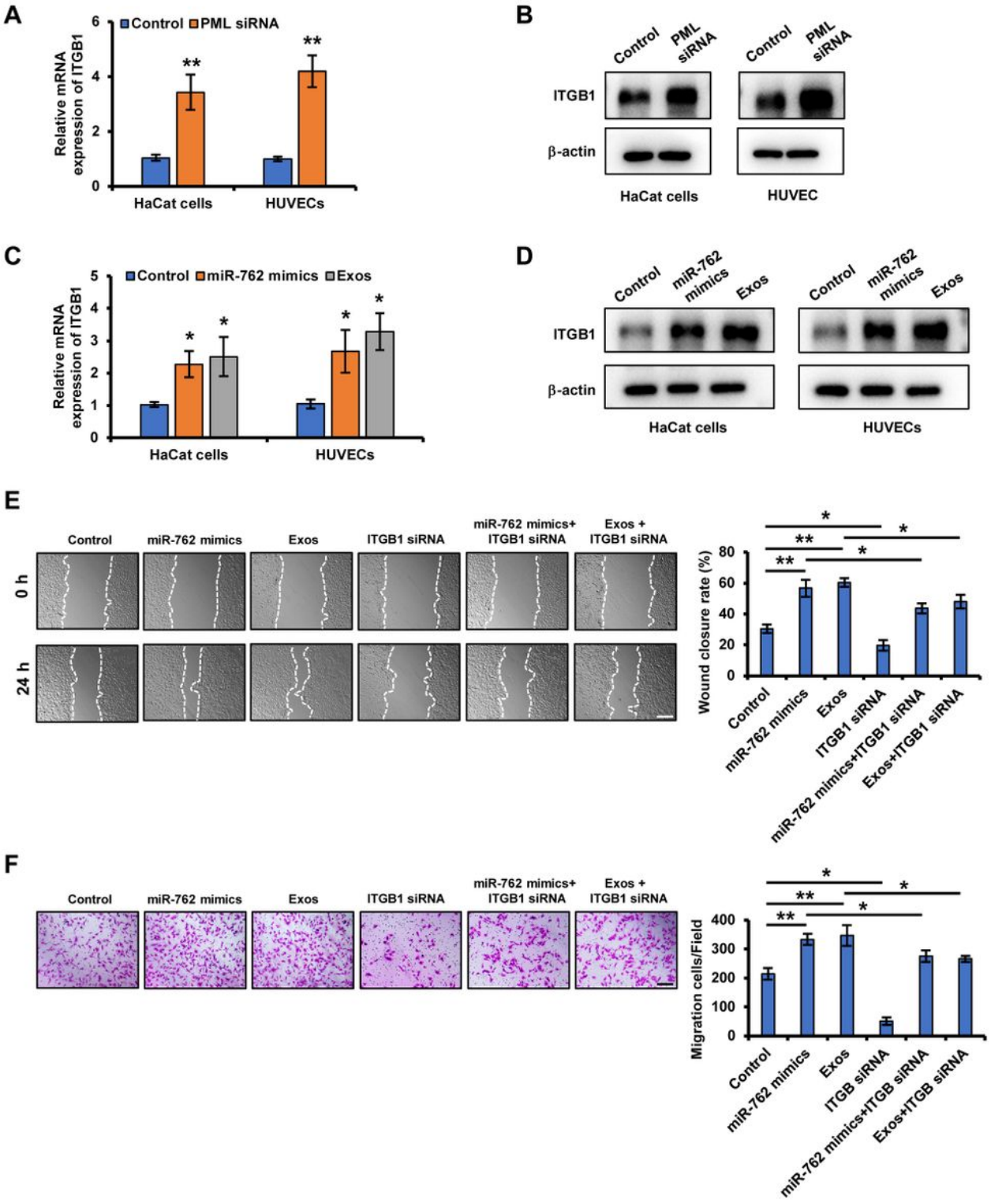

Figure 6

PML regulated ITGB1 is involved in the promotion of keratinocytes and endothelial cell migration by miR-762 and iPSCs-KCs-Exos. qRT-PCR (**A**) and Western blot (**B**) analysis of ITGB1 expression in HaCaT cells and HUVECs which were treated with control siRNA or PML siRNA. qRT-PCR (**C**) and Western blot (**D**) analysis of ITGB1expression in HaCaT cells and HUVECs which were treated with control, miR-762 mimics, iPSCs-KCs-Exos. (**E**) Representative images of the wound healing assay of HaCaT cells and

quantitative analysis of the wound healing rates in each group in each group. Scale bar, 200 μm. (**F**) Images of migrated HUVECs and quantitative analysis of the migrated cells in each group. Scale bar, 200 mm. **P* < 0.05, ***P* < 0.01.